

Evaluation of the properties of natural rubber bio composite and guava residue (*Psidium guajava* L.) as sustainable application

Carlos T. Hiranobe^a , Alex R. da Silva^a, Marco A. G. Cruz^a, João C. S. Canhada^a, Samara S. Araújo^a, José A. Rocha^a, Harison F. dos Santos^a, Gabriel D. Ribeiro^a, Gabrieli R. Tolosa^b, Gleyson T. A. Santos^b, Eduardo R. Budemberg^a, Cláudia G. de Azevedo^a, Renivaldo J. dos Santos^{a*} 

^aUniversidade Estadual Paulista (UNESP), Faculdade de Engenharia e Ciências, Departamento de Engenharia de Energia, Avenida dos Barrageiros, 19274-000, Rosana, SP, Brasil.

^bUniversidade Estadual Paulista (UNESP), Faculdade de Ciência e Tecnologia, Departamento de Física, Rua Roberto Simonsen, 19060-900, Presidente Prudente, SP, Brasil.

Received: December 03, 2022; Revised: June 01, 2023; Accepted: July 19, 2023

In juice and pulp extraction, about 10% of fruit waste is generated, which often ends up in landfills that can cause environmental damage, serve as food for insects and rodents, and cause health problems for humans. In this work, micronized guava waste was used as a filler in vulcanized compounds in natural rubber. Mechanical properties such as hardness, tensile strength, tear resistance, and abrasion resistance were evaluated, as well as thermal properties such as thermogravimetric analysis, in addition to scanning electron microscopy, X-ray fluorescence, elemental analysis, and infrared spectroscopy. According to the results of the mechanical properties tests, the addition of up to 20 phr of the filler tends to improve the tensile strength of the composites, resulting in an increase in the density of cross-links obtained through the Flory-Rehner method. The thermal behavior analyzed by TGA and FTIR spectra were not affected by the incorporation of fillers.

Keywords: *Natural rubber, bio composite, lignocellulosic biomass, guava, sustainability.*

1. Introduction

The guava fruit (*Psidium guajava* L.) is notable in the food and trade industries due to its high orchard productivity - in Brazil, an average of 578,000 tons of guava are produced annually - and its rich nutritional value as a source of vitamin C, vitamin B6, lycopene, potassium, copper, fiber, and antioxidants. India is the world's leading producer of white guava¹. Although the fruit is popular for consumption in its natural state, it ripens and spoils quickly, leading to the majority of production being processed industrially to manufacture juices, pulps, jams, nectars, yogurts, and sweet and sour sauce². In the pulp processing procedure, approximately 8% to 10% of residues are generated, comprising seeds, peels, pulp, and fibrous materials, which are used as animal feed or frequently disposed of in landfills³.

The development of composites reinforced with natural rubber fibers presents a potential solution to both technological and environmental challenges⁴. Lignocellulosic biomass fibers are comprised of three structural components - hemicellulose, cellulose, and lignin - and possess numerous inherent advantages, such as being non-abrasive, requiring low energy consumption, offering high specific properties, having low density and cost, and being biodegradable when compared to synthetic fibers⁵. The most extensively studied plant fibers include jute⁶, flax⁷, hemp⁸, sisal⁹, pineapple¹⁰, coconut¹¹, cotton¹², rice straw¹³, wood, and roots¹⁴.

The application of guava residue can be found in the literature in the form of biochar as an adsorbent for polycyclic aromatic hydrocarbons¹⁵, as an adsorbent for As³⁺ in wastewater¹⁶, and in gasification for the generation of hydrocarbons¹⁷.

In recent years, the development of lignocellulosic biocomposite materials has been observed, using natural rubber as the polymer matrix with alkalized wheat straw to resist fire¹⁸, silanized cereal straws to increase mechanical and fire resistance¹⁹, and black spruce (conifer) cellulose pulps to partially replace carbon black without affecting the quality of its mechanical properties²⁰. The advanced application of matrix/filler composites is based on the study of their physical properties in conjunction with their mechanical, thermal, and electrical properties. Additionally, environmental concerns surrounding their production aim to reduce environmental impacts²¹.

In this work, we obtained a new composite formed by natural rubber and guava residue and evaluated its mechanical, thermal, morphological, and structural properties.

2. Experimental Process

2.1. Material

Natural rubber (NR) of Brazilian light-colored crepe (CCB) type was acquired from DLP Indústria e Comércio de Borracha e Artefatos LTDA (São Paulo, Brazil). Guava

*e-mail: renivaldo.santos@unesp.br

fruit biomass was produced in the laboratory; firstly, the biomass underwent the grinding and filtration process to separate the biomass from the juice, and then it was dried in an oven at a temperature of 104 °C. After drying, the residue was micronized until obtaining a particle size smaller than 30 mesh. Other reagents were commercially acquired, with a high degree of purity, and used without any pre-treatment, such as activation agents (zinc oxide and stearic acid), curing agent (sulfur), antioxidant (vulcanox), plasticizers (processing oil and polyethylene glycol/PEG 4000), and vulcanization accelerators (benzothiazole disulfide/MBTS and tetramethylthiuram disulfide/TMTD).

2.2. Preparation of the composites

The composites were prepared in two stages. In the first stage, the proportions of guava biomass (0, 10, 20, 30 and 40 phr) and the amount of reagents to be incorporated into the natural rubber were defined based on established parameters. The formulation used in the preparation of the composites is shown in Table 1. Next, the natural rubber was masticated in the open roll mill of the Makintec brand, model 379 m, at 65 °C and a friction ratio of 1:1.25. After rubber mastication for approximately 20 minutes, the activation and processing agents (zinc oxide, stearic acid, polyethylene glycol, vulcanox and processing oil) and the filler (guava residue) were incorporated. In the second stage, the cross-linking agent (sulfur) and the vulcanization accelerators (benzothiazole disulfide/MBTS and tetramethylthiuram disulfide/TMTD) were incorporated, according to ASTM D3182 standard²².

In this work, the semi-efficient vulcanization (SEV) system was chosen because it provides intermediate mechanical properties. Thus, it would be easier to evaluate if guava waste offers any improvement in the mechanical properties of the composites.

2.3. Methodology

2.3.1. Rheometric properties

The rheometric properties were obtained using the MDR 2000 oscillating disk rheometer from Team Equipamentos with an oscillating angle of 1° and at a temperature of 150 °C, in accordance with ASTM D2084²³. The composites were vulcanized in a hydraulic press under a pressure of 3.0 MPa

Table 1. Formulation of natural rubber and guava residue.

Components	Components quantities in phr*				
	NR/G ₀	NR/G ₁₀	NR/G ₂₀	NR/G ₃₀	NR/G ₄₀
NR (CCB)	100	100	100	100	100
Zinc oxide	5	5	5	5	5
Stearic acid	2	2	2	2	2
PEG 4000	0	2	2	2	2
antioxidant vulcanox	0	1,5	1,5	1,5	1,5
Processing oil	0	3	3	3	3
guava waste	0	10	20	30	40
sulphur	1.5	1.5	1.5	1.5	1.5
accelerator MBTS	1	1	1	1	1
accelerator TMTD	0.5	0.5	0.5	0.5	0.5

*phr (per hundred rubber); NR/G (Natural Rubber/Guava residue).

at 150 °C, using the optimal cure time (t_{90}) obtained from rheometry, so that all composites had the same degree of cure.

2.3.2. Degree of dispersion of fillers in the polymer matrix

The degree of dispersion of guava residue in natural rubber compounds can be quantitatively determined by Equation 1²⁴:

$$L = \eta_r - m_r = \frac{M_{Lc}}{M_{Lg}} - \frac{M_{Hc}}{M_{Hg}} \quad (1)$$

Where L is the degree of dispersion of the filler in the polymer matrix; η_r is the ratio $[M_{Lc}/M_{Lg}]$; m_r is the ratio $[M_{Hc}/M_{Hg}]$; M_L is the minimum torque; M_H is the maximum torque; c and g represent the filler and pure gum, respectively.

2.3.3. Density

The determination of the density of the composites was obtained according to ASTM D297²⁵ using ethyl alcohol with a density of 0.79 g·cm⁻³ and calculated by Equation 2:

$$\rho = \frac{\rho_L \cdot m_A}{m_A} + \frac{m_B}{m_B} \quad (2)$$

Where ρ is the density of the sample (g·cm⁻³); ρ_L represents the density of ethanol at the analysis temperature (g·cm⁻³); m_A is the mass of the sample without wire in air (g) and the m_B is the mass of the sample without wire in liquid (g).

2.3.4. Cross-linking density by swelling method and Flory-Rehner equation

The cross-linking densities were estimated by the equilibrium swelling technique in organic solvent, using Equation 3 developed by Flory and Rehner²⁶. In this technique, the samples were weighed to a mass of approximately 0.25 ± 0.05 g and immersed in toluene in the dark for 5 days until equilibrium was reached. The samples were then removed, dried to remove excess solvent, and weighed. Next, the samples were placed in an oven at a temperature of 80 °C for 24 hours and weighed. The values used for the molar volume of toluene (V_0) and for the Flory-Huggins interaction parameter ($\chi_{\text{Toluene,NR}}$) for natural rubber and toluene were 106.3 cm³·mol⁻¹ and 0.393 respectively.

$$v = \frac{-\ln(1 - V_B) + V_B + \chi_{\text{Toluene,NR}}(V_B)^2}{(\rho_B)(V_0) \left(\frac{1}{V_B^2} - \frac{V_B}{2} \right)} \quad (3)$$

Where v is the cross-link density (mol·cm⁻³); ρ_B is the density rubber (g·cm⁻³) e V_B is the volume fraction of rubber in the swollen form, determined from the weight increase by swelling.

2.3.5. Scanning electron microscopy (SEM)

The Carl Zeiss EVO LS15 scanning electron microscopy equipment at 20 kV was used to investigate the surface morphology of fractured composites. The samples were coated with a thin layer of gold using a Quorum Q 150R ES sputter coater. The chemical elements present at a particular point on the material were identified by energy dispersive X-ray spectroscopy (EDX).

2.3.6. X-ray fluorescence (XRF)

The presence of inorganic compounds was determined using an energy dispersive X-ray fluorescence spectrometer Shimadzu EDX-7000/8000/8100.

2.3.7. Elemental organic analysis (CHNSO)

The elemental compositions of the samples were determined from the masses of 2 to 3 mg of dry sample, in triplicate, using the Thermo Scientific Flash AE 1112 elemental analyzer. The basic operating principle of this equipment is to separate the gases generated in the form of CO_2 , N_2 , H_2O e H_2SO_3 , which are carried by helium gas in a column and detected by thermal conductivity. This equipment identifies the contents of (C), hydrogen (H), nitrogen (N), sulphur (S) and oxygen (O).

2.3.8. Fourier transform infrared spectroscopy (FTIR)

FTIR spectroscopy was performed using a Bruker Vector 22 spectrometer in the attenuated total reflectance (ATR) mode, in the range of 4000-400 cm^{-1} with a spectral resolution of 4 cm^{-1} and 32 scans.

2.3.9. Test of resistance to tearing

Resistance to tear tests were performed on the Instron/Emic DL2000 universal testing machine at 500 $\text{mm}\cdot\text{min}^{-1}$ with a 5 kN load cell and an internal strain transducer. For these tests, quintuplicate specimens of type C test pieces (test pieces with right angles) were used, in accordance with ASTM D624 standard²⁷.

2.3.10. Stress-Strain test

Tensile strength tests were performed on the Instron/Emic DL2000 universal testing machine at 500 $\text{mm}\cdot\text{min}^{-1}$ with a 5 kN load cell and an internal strain transducer. For these tests, type A specimens (straight section and dumbbell specimens) were used, according to ASTM D412 standard²⁸.

2.3.11. Hardness test

The determination of surface hardness of the composites was obtained according to ASTM D2240 standard²⁹ on the Shore A scale, using an analog Digimess durometer with a capacity of 0 to 100 and a 1 Shore A graduation.

2.3.12. Test of resistance to abrasion

The abrasion loss was calculated using Equation 4, according to ASTM D5963 standard³⁰, using the MaqTest equipment with an abrasion course equivalent to 40 m and a pressure on the test specimen against the cylinder of 5 N.

$$PA = \frac{\Delta m S_0}{\rho S} \quad (4)$$

Where PA represents the abrasion loss ($\text{mm}^3 / 40 \text{ m}$); Δm is the mass loss of the composite (mg); S_0 is the theoretical attack index of sandpaper on standard rubber ($200 \pm 20 \text{ mg}$); S is the actual attack index of sandpaper on standard rubber (mg) and ρ is the density of the composite ($\text{mg}\cdot\text{mm}^{-3}$).

2.3.13. Thermogravimetric analysis (TGA)

The Thermogravimetric Analysis (TGA) tests were performed on a NETZSCH equipment model 209, with a temperature range from around 25 °C to 900 °C, using a heating rate of 10 °C·min⁻¹ under a nitrogen atmosphere with a flow rate of 15 mL·min⁻¹. The amount of sample used for the measurements was approximately 10 mg, according to ASTM D6370 standard³¹.

3. Results and Discussion

3.1. Rheological properties of composites

Figure 1 illustrates the rheometry curves of the composites, and Table 2 presents the values of the minimum (M_L) and maximum (M_H) torques, torque variation (ΔM), pre-curing or safety time (t_s), optimal curing time (t_{90}) and cure rate index (CRI).

The values of the minimum and maximum torques slightly increased with the increase in the amount of guava waste. The increase in the maximum torque values for higher waste contents indicates that the presence of fillers in the polymeric matrix reduces the mobility of the polymer chains. The torque variation is related to the stiffness of the vulcanized material, which in turn is related to the degree of crosslinking and the presence of fillers. Therefore, the increase in torque variation suggests an increase in crosslink density with increasing filler content. By means of the swelling technique, good interaction between the filler and the matrix was observed,

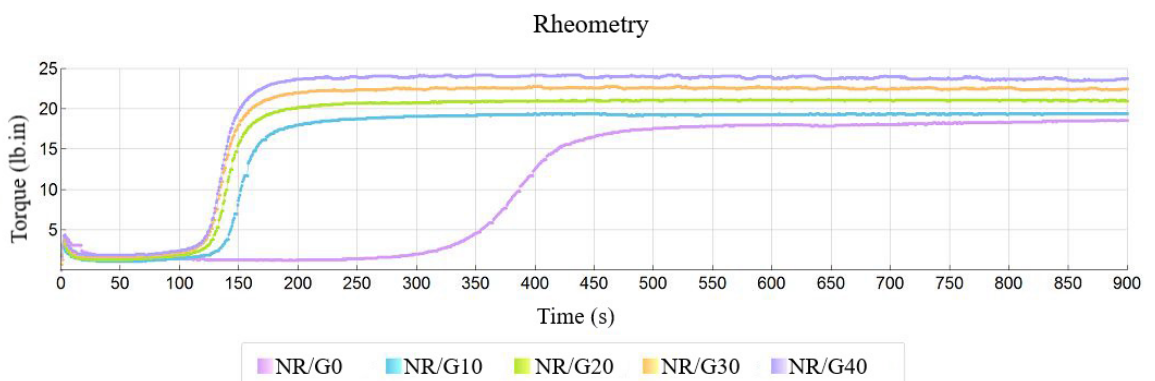


Figure 1. Rheometry curves of natural rubber and guava waste composites.

since the filler prevents solvent penetration, behaving as if they were cross-linking points. As the swelling technique performed is only quantitative and not qualitative, there is an increase in the cross-link density when considering these interaction points as cross-linking.

One can observe from Table 2 that the (t_s) and (t_{90}) decreased significantly with the addition of fillers, as shown in Table 3 regarding the chemical composition of guava waste, the presence of metal oxides can increase the cure rate. By increasing the amount of filler, the content of metal oxides in rubber blends also increases, contributing to this increase in the vulcanization rate. The addition of metal oxide increases the reactive sulfur complexes, which consequently raises the degree of crosslinking. In the vulcanization of natural rubber (NR), elemental sulfur is activated by the presence of metal oxide and fatty acid, forming the metallic stearate. Several studies report activation and increased cure rate with the presence of metal oxides^{32,33,34}. Additionally, the addition of chemical agents such as PEG 4000, antioxidant, and processing oil, incorporated in the filled composites, may have also influenced the processing times of the vulcanized rubber.

The reduction in vulcanization time of the filled composites also led to a decrease in the cure rate index, resulting in a faster curing rate.

3.2. Degree of dispersion of fillers in the polymer matrix

Based on the data of minimum and maximum torque properties shown in Table 2, the values of L for the dispersion of guava residue in the natural rubber matrix are shown in

Table 2. Rheometric parameters of NR/G composites.

Composites	M_L	M_H	$\Delta M = (M_H - M_L)$	t_s	t_{90}	CRI = $100/(t_{90} - t_s)$
NR/G	(dNm)	(dNm)	(dNm)	(min)	(min)	(min ⁻¹)
0 phr	1.24 ± 0.06	20.43 ± 0.61	19.19 ± 0.62	4.98 ± 0.09	7.00 ± 0.46	49.67 ± 9.25
10 phr	1.36 ± 0.11	21.32 ± 0.62	19.96 ± 0.62	1.93 ± 0.15	2.75 ± 0.35	121.62 ± 26.59
20 phr	1.58 ± 0.11	23.54 ± 0.36	21.96 ± 0.46	1.86 ± 0.03	2.67 ± 0.19	123.29 ± 22.83
30 phr	1.73 ± 0.13	25.12 ± 0.56	23.39 ± 0.49	1.81 ± 0.03	2.64 ± 0.13	120.81 ± 17.06
40 phr	2.03 ± 0.11	26.93 ± 0.40	24.89 ± 0.35	1.78 ± 0.06	2.58 ± 0.12	125.87 ± 9.64

Table 3. Chemical composition of the constituents of guava residue obtained from X-ray fluorescence (XRF) and by elemental organic analysis.

X-Ray Fluorescence		Elemental Analysis	
Chemical composition	Quantities (%)	Elements	Quantities (%)
K ₂ O	2.11	C	46.24 ± 0.44
SO ₃	1.343	H	7.36 ± 0.07
P ₂ O ₅	1.04	N	1.46 ± 0.12
MgO	0.6	O	42.38 ± 0.31
SiO ₂	0.489	S	2.55 ± 0.15
CaO	0.353	---	---
CuO	0.011	---	---
Fe ₂ O ₃	0.01	---	---
ZnO	0.005	---	---
MnO	0.004	---	---
CO ₂	94.035	---	---
Total	100	Total	100

Figure 2. A lower value of L, for a given filler, compared to the unfiller composite, indicates a better degree of residue dispersion. The degree of filler dispersion was adequate up to the incorporation of 30 phr of residue, while at 40 phr, the occurrence of inter-agglomeration between fillers weakens the mechanical properties of the composites. A lower viscosity tends to reduce the minimum torque and facilitate the filler dispersion, strengthening the BN/Guava residue interaction. The filler-matrix interaction can be defined as additional physical crosslinks that contribute to the overall crosslink density³⁵.

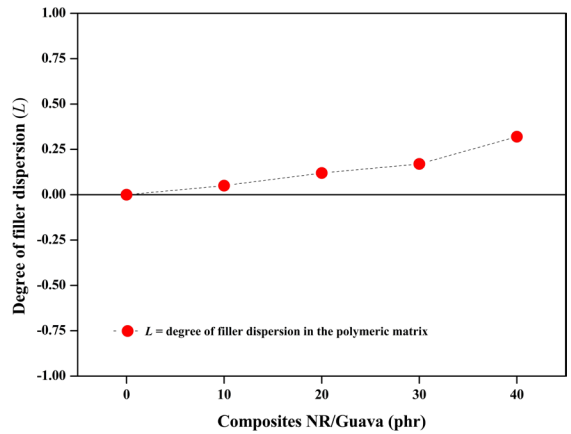


Figure 2. Degree of dispersion of guava residue particles in the natural rubber matrix.

3.3. Scanning electron micrography (SEM) and energy dispersive X-ray spectroscopy (EDX)

The SEM images were taken from the test specimens after tensile deformation tests and are shown in Figure 3. Figure 3a shows a photographic image of dehydrated guava waste, and Figure 3b shows the scanning electron micrograph of guava waste at 1000 \times magnification.

It is possible to observe that the guava waste powder has an amorphous surface area with considerable roughness, favoring the interaction between the filler and the polymer matrix. In Figure 3c, we can observe that the surface area of the unfilled composite is very rough, while in Figure 3d of its fracture, the presence of grooves and vulcanization

reagents can be seen. With the incorporation of fillers, in Figure 3e, 3g, 3i, and 3k, it can be noted that the surface areas became smoother, with punctual presence of fillers encapsulated by the polymer matrix. In the images of the fracture surfaces of the composites, Figure 3f, 3h, 3j, and 3l, it can be observed that the fillers adhered well to the elastomeric matrix, proving that the roughness of the guava waste favored the matrix/filler interaction.

The Figure 4a1 and 4b1 present the test areas of energy dispersive X-ray spectroscopy (EDX) spectra of the chemical elements constituting the natural rubber composites without filler, Figure 4a2, and with 10 phr of guava waste, Figure 4b2. In Figure 4a2, which refers to the composite without filler, we can observe that the analyzed area consists of 64.41%

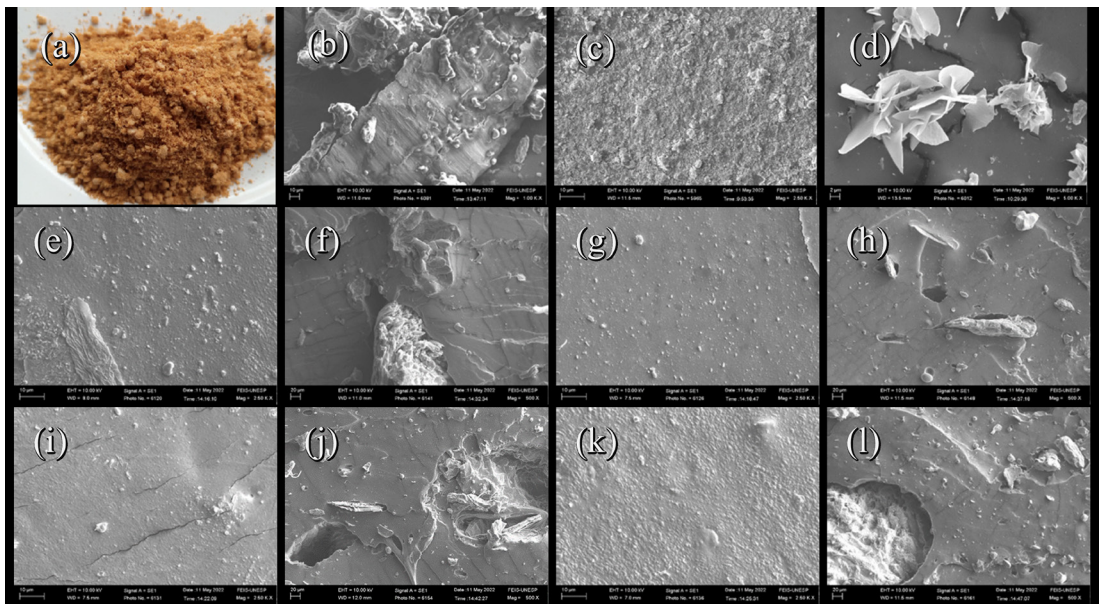


Figure 3. Imagens of guava residue (a) photographic image of dehydrated guava residue, (b) SEM - guava waste powder, (c) SEM - surface NR/G 0phr, (d) SEM - fracture NR/G 0phr, (e) SEM - surface NR/G 10phr, (f) SEM - fracture NR/G 10phr, (g) SEM - surface NR/G 20phr, (h) SEM - fracture NR/G 20phr, (i) SEM - surface NR/G 30phr, (j) SEM - fracture NR/G 30phr, (k) SEM - surface NR/G 40phr and (l) SEM - fracture NR/G 40phr.

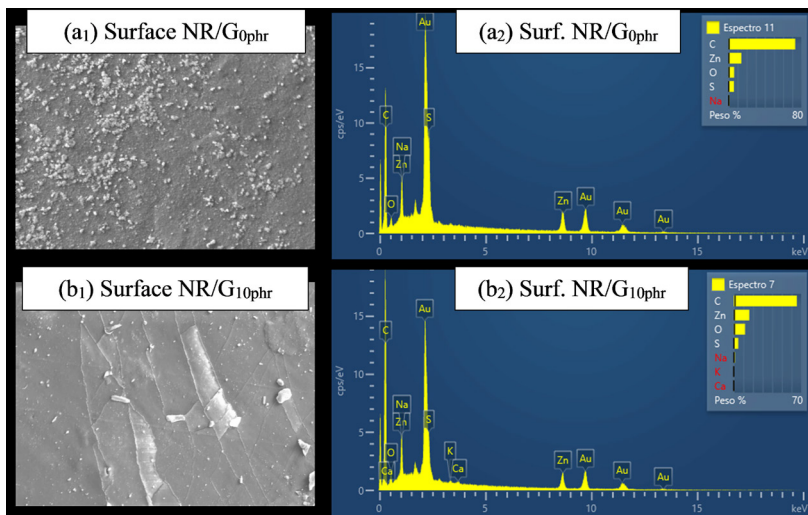


Figure 4. Energy dispersive X-ray spectroscopy of the unfilled (a₂) and 10 phr (b₂) guava waste powder NR composites.

carbon and 5.08% oxygen, coming from the constitution of the natural rubber; 17.25% zinc oxide and 12.11% sulfur, coming from the vulcanizing additives as activation and crosslinking agents, respectively; and still 1.15% sodium, probably from the processing oil added in the formulation of natural rubber. In Figure 4b2, we observe the presence of all the aforementioned constituents and an additional 0.31% potassium and 0.30% calcium, coming from the chemical composition of the guava waste.

3.4. X-ray fluorescence (XRF) and elemental organic analysis of guava residue.

Table 3 shows the chemical constitution of the guava residues obtained from X-ray fluorescence. The XRF indicates that, in addition to the chemical elements potassium and calcium determined in the EDX assays, guava waste is composed of other inorganic compounds, such as phosphorus, magnesium, copper, iron, rubidium, and manganese.

The organic chemical composition by elemental analysis was carried out to complement the XRF results, and its values are shown in Table 3. The results obtained by the elemental analyzer show that the chemical elements present in greater quantities in the guava biomass are carbon and oxygen, a result similar to that found by XRF. Hydrogen and sulfur also appear in significant amounts in the composition of guava.

3.5. Density, hardness (shore A), and abrasion resistance

Table 4 presents the results of density, hardness on the Shore A scale, and abrasion loss tests. All composites had a density above $1 \text{ g}\cdot\text{cm}^{-3}$ and gradually increased with the incorporation of fillers up to a value of $1.09 \text{ g}\cdot\text{cm}^{-3}$ with 40 phr of residue. The hardness values presented in Table 4 are on the hardness grading scale for vulcanized rubbers, considered soft (40 to 60 Shore A) according to ASTM D2240²⁹, and were measured in triplicate samples from different regions of the composite. The incorporation of fillers significantly increased abrasion loss due to the length of the biomass particles and their dispersion in the matrix, which can cause stress points and detachment of the filler during frictional wear.

3.6. Resistance to tearing

Figure 5 shows the bar chart of tear strength for NR/G composites with and without filler (reference), and their values are presented in Table 5. It can be observed that the tear strength of the vulcanized composites remained unchanged with the presence of the fillers, considering the calculated statistical error.

3.7. Stress-Strain test

The Figure 6 shows the tensile strength curves and Table 6 presents the values of tensile strength at rupture. In Table 6, it can be observed that the addition of 20 phr of filler enhances the tensile strength at rupture. However, beyond this threshold, the tensile strength of the composites tends to decrease. While higher filler loadings result in reduced deformation and tensile strength values at rupture, the elasticity modules at 100% and 300% exhibit improvement. This behavior suggests that 20 phr represents the optimal value for reinforcing the filler due to the favorable interaction

between the filler and the matrix. For higher filler loadings, the filler-filler interaction becomes more predominant, thereby increasing rigidity and reducing the stress at rupture.

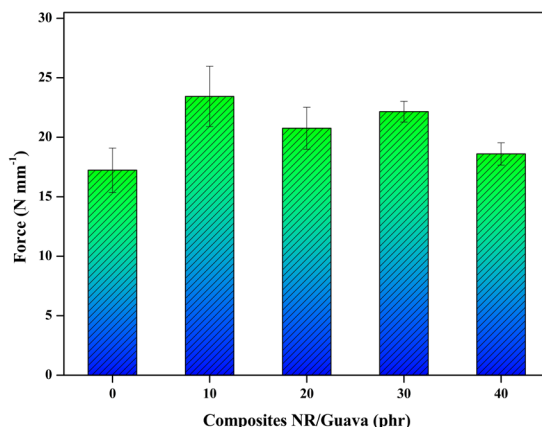


Figure 5. Bar graph of tear strength of NR/G composites.

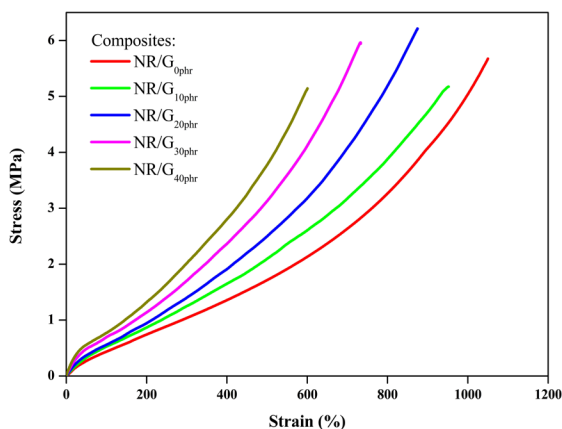


Figure 6. Stress-Strain curves of NR/G.

Table 4. Density, Hardness (Shore A) and Abrasion loss of NR/G composites.

Composites	Density (g cm^{-3})	Hardness (Shore A)	Abrasion loss ($\text{mm}^3 / 40 \text{ m}$)
NR/G _{0phr}	1.01	44 ± 0	220.33 ± 0.34
NR/G _{10phr}	1.04	45 ± 0	373.21 ± 11.00
NR/G _{20phr}	1.06	46 ± 0	335.38 ± 5.97
NR/G _{30phr}	1.08	49 ± 1	350.62 ± 0.93
NR/G _{40phr}	1.09	51 ± 1	395.09 ± 14.31

Table 5. Table of tear resistance values.

Composites	Force (N·mm ⁻¹)	Strain (%)
NR/G _{0phr}	17.23 ± 1.86	353 ± 24
NR/G _{10phr}	23.43 ± 2.54	592 ± 22
NR/G _{20phr}	20.76 ± 1.76	538 ± 18
NR/G _{30phr}	22.15 ± 0.87	578 ± 19
NR/G _{40phr}	18.6 ± 0.94	480 ± 15

Table 6. Table of values of tensile strength at break of NR/G composites.

Composites	Stress at break (MPa)	Strain at break (%)	Module of elasticity (GPa)	Module at 100% (MPa)	Module at 300% (MPa)
NR/G _{0p}	4.54 ± 0.88	1050 ± 12	0.005	0.44	1.04
NR/G _{10p}	5.17 ± 0.54	952 ± 9	0.005	0.50	1.24
NR/G _{20p}	6.21 ± 0.33	875 ± 14	0.008	0.56	1.40
NR/G _{30p}	5.96 ± 0.64	733 ± 11	0.010	0.72	1.72
NR/G _{40p}	5.14 ± 0.27	600 ± 7	0.019	0.81	2.12

Table 7. Cross-link density by swelling method (Flory-Rehner).

Composites	Cross-link density $\nu \times 10^{-4}$ (mol cm ⁻³)
NR/G _{0p}	1.24
NR/G _{10p}	1.34
NR/G _{20p}	1.39
NR/G _{30p}	1.44
NR/G _{40p}	1.45

Table 8. Identification of the infrared spectra of guava residue and natural rubber.

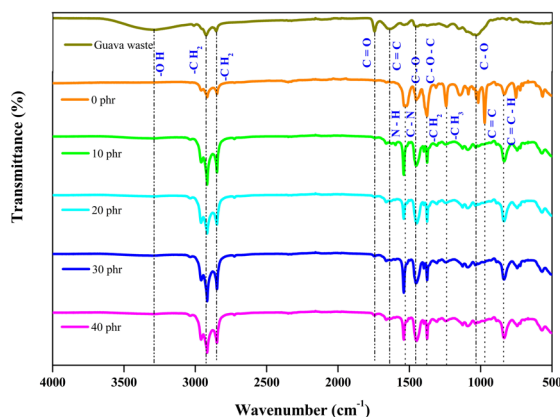
Guava fruit residue, dried and micronized		
Wavenumber (cm ⁻¹)	Attributions	References
3290	O-H stretching	37
2926	-CH ₂ - asymmetric stretching	38
2849	-CH ₂ - symmetric stretching	38
1744	C=O stretching	38
1641	C=O and C=C stretching	37,38
1454	C-O and C-O-C stretching	37
1033	C-O stretching	37
Natural rubber		
2926	-CH ₂ - asymmetric stretching	39
2849	-CH ₂ - symmetric stretching	39
1540	Amide II: Bending in the N-H plane and C-N stretching (proteins)	39,40
1450	Angular deformation of -CH ₂ - and swing type vibration of -CH ₃	39,41
1375	-CH ₃ asymmetric deformation	39
1240	C-O-C symmetric stretching and -CH ₂ - torsion	42
971	C=C torsion	39
834	C=C-H out of plane bending	39

3.8. Cross-linking density – Flory-Rehner

The determination of cross-link density by the swelling method in organic solvent using the Flory-Rehner equation is the simplest, practical, and economical methodology that provides good results³⁶. Table 7 shows the obtained values of the cross-link densities using toluene as the organic solvent. We can observe that the cross-link densities increase gradually with the incorporation of fillers, corroborating with the results of torque variations presented in Table 2.

3.9. Fourier transform infrared spectra analysis

The chemical composition of guava waste and its vulcanized composites, evidenced by functional groups, are presented in the infrared spectra of Figure 7 and identified in Table 8.

**Figure 7.** Infrared spectra of NR/G composites.

The composites with fillers presented all similar functional groups, confirming that the interaction between polymer matrix and filler occurs physically without generating new spectral bands.

3.10. Thermogravimetric analysis (TGA)

The results of the TGA and DTG curves obtained from the guava waste powder and its composites are shown in Figure 8a and 8b. Four mass loss events were observed. The first mass loss occurs at a temperature close to 86 °C and corresponds to 1% of the total weight of the composite, being attributed to the loss of water and low thermal stability volatile materials. The second mass loss of approximately 4%, evidenced at a temperature close to 187 °C, corresponds to the decomposition of hemicellulose. The third event occurs at a temperature close to 260 °C and is attributed to the decomposition of cellulose, corresponding to 13% of the mass loss. The last event presents a mass loss of around 77% and corresponds to the overlap of lignin degradation with BN, occurring at temperatures of 318 °C and 347 °C, respectively^{43,44}. The residual mass, about 3 to 5%, is attributed to the inorganic compounds present in the sample (potassium, calcium, phosphorus, magnesium, silica, copper, iron, and zinc) and the chemical additives added in the vulcanization process such as zinc from zinc oxide.

4. Conclusion

In this article, the feasibility of producing a vulcanized biocomposite using micronized guava waste as a filler in a natural rubber matrix was demonstrated. The presence of these fillers in rheometric tests significantly reduced curing time and improved material processability, suggesting energy savings for the crosslinking of rubber composites

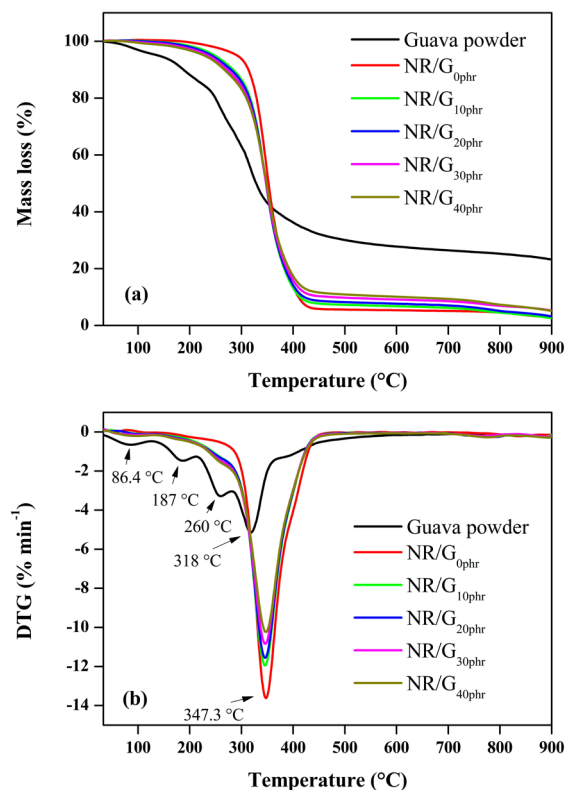


Figure 8. (a) TG curves of guava residue powder and its composites and (b) DTG curves of guava residue powder and its composites.

with fillers. Furthermore, the tensile strength was enhanced with the addition of up to 20 phr of the filler, resulting in an increase in the density of cross-links obtained through the Flory-Rehner method. This allows for the application of the material in rubberized floors and shoe soles. Thermal analysis performed by TGA and FTIR spectra were not affected by the incorporation of the filler, conferring thermal stability to the composite. Scanning electron microscopy demonstrated good interaction between the polymer matrix and the filler. Therefore, this article proves that guava waste can be used as a raw material in rubber artifacts, improving rubber properties performance, generating added value, and reducing environmental impacts.

5. Acknowledgements

The authors would like to thank the Fundação de Amparo à Pesquisa do Estado de São Paulo (FAPESP) for financial support n° 2016/03208-0, and POSMAT-CAPES-PROEX-UNESP for academic assistance.

6. References

- Pereira BS, Freitas C, Vieira RM, Brienza M. Brazilian banana, guava, and orange fruit and waste production as a potential biorefinery feedstock. *J Mater Cycles Waste Manag.* 2022;24(6):2126-40. <http://dx.doi.org/10.1007/s10163-022-01495-6>.
- Angulo-López JE, Flores-Gallegos AC, Torres-León C, Ramírez-Guzmán KN, Martínez GA, Aguilar CN. Guava (*Psidium guajava* L.) fruit and valorization of industrialization by-products. *Processes.* 2021;9(6):1075. <http://dx.doi.org/10.3390/pr9061075>.
- Jan S, Thakur P, Chauhan D, Kaur J. Guava wastes and by-products. In: Muzaffar K, Sofi SA, Mir SA, editors. *Handbook of fruit wastes and by-products: chemistry, processing technology, and utilization.* Boca Raton: CRC Press; 2022. p. 99-111. <http://dx.doi.org/10.1201/9781003164463>.
- Rangappa SM, Siengchin S, Parameswaranpillai J, Jawaid M, Ozbakkaloglu T. Lignocellulosic fiber reinforced composites: progress, performance, properties, applications, and future perspectives. *Polym Compos.* 2022;43(2):645-91. <http://dx.doi.org/10.1002/pc.26413>.
- Asim M, Paridah MT, Chandrasekar M, Shahroze RM, Jawaid M, Nasir M et al. Thermal stability of natural fibers and their polymer composites. *Iran Polym J.* 2020;29:625-48. <http://dx.doi.org/10.1007/s13726-020-00824-6>.
- Rangasamy G, Mani S, Kolandavelu SKS, Alsoufi MS, Ibrahim AMM, Muthusamy S et al. An extensive analysis of mechanical, thermal and physical properties of jute fiber composites with different fiber orientations. *Case Stud Therm Eng.* 2021;28:101612. <http://dx.doi.org/10.1016/j.csite.2021.101612>.
- More AP. Flax fiber-based polymer composites: a review. *Adv Compos Hybrid Mater.* 2022;5(1):1-20. <http://dx.doi.org/10.1007/s42114-021-00246-9>.
- Tanasă F, Zănoagă M, Teacă CA, Nechifor M, Shahzad A. Modified hemp fibers intended for fiber-reinforced polymer composites used in structural applications: a review. I. Methods of modification. *Polym Compos.* 2020;41(1):5-31. <http://dx.doi.org/10.1002/pc.25354>.
- Naveen J, Jawaid M, Amuthakkannan P, Chandrasekar M. Mechanical and physical properties of sisal and hybrid sisal fiber-reinforced polymer composites. In: Jawaid M, Thariq M, Saba N, editors. *Mechanical and physical testing of biocomposites, fibre-reinforced composites and hybrid composites.* Duxford: Woodhead Publishing; 2019. p. 427-40. (Woodhead Publishing Series in Composites Science and Engineering). <https://doi.org/10.1016/B978-0-08-102292-4.00021-7>.
- Todkar SS, Patil SA. Review on mechanical properties evaluation of pineapple leaf fibre (PALF) reinforced polymer composites. *Compos, Part B Eng.* 2019;174:106927. <http://dx.doi.org/10.1016/j.compositesb.2019.106927>.
- Bui H, Sebaibi N, Boutouil M, Levacher D. Determination and review of physical and mechanical properties of raw and treated coconut fibers for their recycling in construction materials. *Fibers.* 2020;8(6):37. <http://dx.doi.org/10.3390/fib8060037>.
- Mathangadeera RW, Hequet EF, Kelly B, Dever JK, Kelly CM. Importance of cotton fiber elongation in fiber processing. *Ind Crops Prod.* 2020;147:112217. <http://dx.doi.org/10.1016/j.indcrop.2020.112217>.
- Alcántara JC, González I, Pareta MM, Vilaseca F. Biocomposites from rice straw nanofibers: morphology, thermal and mechanical properties. *Materials.* 2020;13(9):2138. <http://dx.doi.org/10.3390/ma13092138>.
- Sarikaya E, Çallioğlu H, Demirel H. Production of epoxy composites reinforced by different natural fibers and their mechanical properties. *Compos, Part B Eng.* 2019;167:461-6. <http://dx.doi.org/10.1016/j.compositesb.2019.03.020>.
- Jesus JHF, Matos TTS, Cunha GC, Mangrich AS, Romão LPC. Adsorption of aromatic compounds by biochar: influence of the type of tropical biomass precursor. *Cellulose.* 2019;26:4291-9. <http://dx.doi.org/10.1007/s10570-019-02394-0>.
- Mohan D, Dey S, Dwivedi SB, Shukla SP. Adsorption of arsenic using low cost adsorbents. *Curr Sci.* 2019;117(4):649-61. <http://dx.doi.org/10.18520/cs/v117/i4/649-661>.
- González-Arias S, Zúñiga-Moreno A, García-Morales R, Elizalde-Solis O, Verónico-Sánchez FJ, Flores-Valle SO. Gasification of *psidium guajava* L. Waste using supercritical water: evaluation of feed ratio and moderate temperatures. *Energies.* 2021;14(9):2555. <http://dx.doi.org/10.3390/en14092555>.

18. Rybiński P, Syrek B, Masłowski M, Miedzianowska J, Strzelec K, Żukowski W et al. Influence of lignocellulose fillers on properties natural rubber composites. *J Polym Environ*. 2018;26:2489-501. <http://dx.doi.org/10.1007/s10924-017-1144-9>.
19. Miedzianowska J, Masłowski M, Rybiński P, Strzelec K. Properties of chemically modified (selected silanes) lignocellulosic filler and its application in natural rubber biocomposites. *Materials*. 2020;13(18):4163. <http://dx.doi.org/10.3390/ma13184163>.
20. Kazemi H, Parot M, Stevanovic T, Mighri F, Rodrigue D. Cellulose and lignin as carbon black replacement in natural rubber. *J Appl Polym Sci*. 2022;139(26):e52462. <http://dx.doi.org/10.1002/app.52462>.
21. Girijappa YGT, Rangappa SM, Parameswaranpillai J, Siengchin S. Natural fibers as sustainable and renewable resource for development of eco-friendly composites: a comprehensive review. *Front Mater*. 2019;6:226. <http://dx.doi.org/10.3389/fmats.2019.00226>.
22. ASTM: American Society for Testing and Materials. ASTM D3182-21a: standard practice for rubber: materials, equipment, and procedures for mixing standard compounds and preparing standard vulcanized sheets. West Conshohocken: ASTM; 2021.
23. ASTM: American Society for Testing and Materials. ASTM D2084-19a: standard test method for rubber property: vulcanization using oscillating disk cure meter. West Conshohocken: ASTM; 2019.
24. Lee BL. Reinforcement of uncured and cured rubber composites and its relationship to dispersive mixing: an interpretation of cure meter rheographs of carbon black loaded SBR and cis-polybutadiene compounds. *Rubber Chem Technol*. 1979;52(5):1019-29. <http://dx.doi.org/10.5254/1.3535250>.
25. ASTM: American Society for Testing and Materials. ASTM D297-21: standard test methods for rubber products: chemical analysis. West Conshohocken: ASTM; 2022.
26. Flory PJ, Rehner J Jr. Statistical mechanics of cross-linked polymer networks I. Rubberlike elasticity. *J Chem Phys*. 1943;11(11):512-20. <http://dx.doi.org/10.1063/1.1723791>.
27. ASTM: American Society for Testing and Materials. ASTM D624-00: standard test method for tear strength of conventional vulcanized rubber and thermoplastic elastomers. West Conshohocken: ASTM; 2020.
28. ASTM: American Society for Testing and Materials. ASTM D412-16: standard test methods for vulcanized rubber and thermoplastic elastomers: tension. West Conshohocken: ASTM; 2021.
29. ASTM: American Society for Testing and Materials. ASTM D2240-15: standard test method for rubber property: durometer hardness. West Conshohocken: ASTM; 2021.
30. ASTM: American Society for Testing and Materials. ASTM D5963-04: standard test method for rubber property: abrasion resistance (Rotary Drum Abrader). West Conshohocken: ASTM; 2019.
31. ASTM: American Society for Testing and Materials. ASTM D6370-99: standard test method for rubber: compositional analysis by Thermogravimetry (TGA). West Conshohocken: ASTM; 2019.
32. Ismail HANAFI, Chung FL. The effect of partial replacement of silica by white rice husk ash in natural rubber composites. *Int J Polym Mater*. 1999;43(3-4):301-12. <http://dx.doi.org/10.1080/00914039908009692>.
33. Alam MN, Kumar V, Potiyaraj P, Lee DJ, Choi J. Synergistic activities of binary accelerators in presence of magnesium oxide as a cure activator in the vulcanization of natural rubber. *J Elastomers Plast*. 2022;54(1):123-44. <http://dx.doi.org/10.1177/00952443211020794>.
34. Hayeemasae N, Salleh SZ, Ismail H. Utilization of chloroprene rubber waste as blending component with natural rubber: aspect on metal oxide contents. *J Mater Cycles Waste Manag*. 2019;21:1095-105. <http://dx.doi.org/10.1007/s10163-019-00862-0>.
35. Surya I, Ismail H. The degree of filler dispersion, rheometric and mechanical properties of carbon black-filled styrene-butadiene rubber composites in the presence of alkanolamide. *IOP Conf Ser Mater Sci Eng*. 2019;523:012063. <http://dx.doi.org/10.1088/1757-899X/523/1/012063>.
36. Hiranobe CT, Ribeiro GD, Torres GB, Reis EAPD, Cabrera FC, Job AE et al. Cross-linked density determination of natural rubber compounds by different analytical techniques. *Mater Res*. 2021;24:e20210041. <http://dx.doi.org/10.1590/1980-5373-MR-2021-0041>.
37. Kumar KV, Pillai MSN, Thusnavis GR. Seed extract of *Psidium guajava* as ecofriendly corrosion inhibitor for carbon steel in hydrochloric acid medium. *J Mater Sci Technol*. 2011;27(12):1143-9. [http://dx.doi.org/10.1016/S1005-0302\(12\)60010-3](http://dx.doi.org/10.1016/S1005-0302(12)60010-3).
38. Joseph CG, Bono A, Krishnaiah D, Soon KO. Sorption studies of methylene blue dye in aqueous solution by optimised carbon prepared from guava seeds (*Psidium guajava* L.). *Mater Sci*. 2007;13:83-7.
39. Rolere S, Liengprayoon S, Vaysse L, Sainte-Beuve J, Bonfils F. Investigating natural rubber composition with Fourier Transform Infrared (FT-IR) spectroscopy: a rapid and non-destructive method to determine both protein and lipid contents simultaneously. *Polym Test*. 2015;43:83-93. <http://dx.doi.org/10.1016/j.polymertesting.2015.02.011>.
40. Nallasamy P, Mohan S. Vibrational spectra of cis-1, 4-polyisoprene. *Arab J Sci Eng*. 2004;29(1A):17-26.
41. Dinsmore HL, Smith DC. Analysis of natural and synthetic rubber by infrared spectroscopy. *Anal Chem*. 1948;20(1):11-24. <http://dx.doi.org/10.5254/1.3542981>.
42. Salaeh S, Nakason C. Influence of modified natural rubber and structure of carbon black on properties of natural rubber compounds. *Polym Compos*. 2012;33(4):489-500. <http://dx.doi.org/10.1002/pc.22169>.
43. Silveira-Junior EG, Perez VH, Justo OR, David GF, Simionatto E, Oliveira LCS. Valorization of guava (*Psidium guajava* L.) seeds for levoglucosan production by fast pyrolysis. *Cellulose*. 2021;28:71-9. <http://dx.doi.org/10.1007/s10570-020-03506-x>.
44. Tapangnoi P, Sae-Oui P, Naebpetch W, Siriwong C. Preparation of purified spent coffee ground and its reinforcement in natural rubber composite. *Arab J Chem*. 2022;15(7):103917. <http://dx.doi.org/10.1016/j.arabjch.2022.103917>.